
Reducing Overestimation Bias by Increasing Representation Dissimilarity in Ensemble Based Deep Q-Learning

Hassam Ullah Sheikh

Department of Computer Science
University of Central Florida
hassam.sheikh@knights.ucf.edu

Ladislau Bölöni

Department of Computer Science
University of Central Florida
lboloni@cs.ucf.edu

Abstract

The first deep RL algorithm, DQN, was limited by the overestimation bias of the learned Q-function. Subsequent algorithms proposed techniques to reduce this problem, without fully eliminating it. Recently, the Maxmin and Ensemble Q-learning algorithms used the different estimates provided by ensembles of learners to reduce the bias. Unfortunately, in many scenarios the learners converge to the same point in the parametric or representation space, falling back to the classic single neural network DQN. In this paper, we describe a regularization technique to increase the dissimilarity in the representation space in these algorithms. We propose and compare five regularization functions inspired from economics theory and consensus optimization. We show that the resulting approach significantly outperforms the Maxmin and Ensemble Q-learning algorithms as well as non-ensemble baselines.

1 Introduction

Q-learning [1] and its deep learning based successors inaugurated by DQN [2] are model-free, value function based reinforcement learning algorithms. Their popularity stems from their intuitive, easy-to-implement update rule derived from the Bellman equations. At each time step, the agent updates its Q-value towards the expectation of the current reward plus the value corresponding to the maximal action in the next state. This state-action value represents the maximum sum of reward the agent believes it could obtain from the current state by taking the current action. Unfortunately [3, 4] have shown that this simple rule suffers from *overestimation bias*: due to the maximization operator in the update rule, upwards and downwards errors do not cancel each other out, but upwards errors accumulate. The overestimation bias is particularly problematic under function approximation and have contributed towards learning sub-optimal policies [3, 5, 6].

A possible solution is to introduce *underestimation* bias in the estimation of the Q-value. Double Q-learning [4] maintains two independent state-action value estimators (Q-functions). The state-action value of estimator one is calculated by adding observed reward and maximal state-action value from the other estimator. Double DQN [7] applied this idea using neural networks, and was shown to provide better performance than DQN. More recent actor-critic type deep RL algorithms such as TD3 [8] and SAC [9] also use two Q function estimators (in combination with other techniques).

Other approaches such as EnsembleDQN [10] and MaxminDQN [11] maintain *ensembles* of Q-functions to estimate an unbiased Q-function. EnsembleDQN estimates the state-action values by adding the current observed reward and the maximal state-action value from the average of Q-functions from the ensemble. MaxminDQN creates a proxy Q-function by selecting the minimum Q-value for each action from all the Q-functions and using the maximal state-action value from

the proxy Q-function to estimate an unbiased Q-function. Both EnsembleDQN and MaxminDQN have been shown to perform better than Double DQN. The primary insight of this paper is that the performance of ensemble based methods is *contingent on maintaining sufficient dissimilarity in the representation space* between the Q-functions in the ensembles. If the Q-functions in the ensembles converge to a common representation (and indeed, in this paper we will show that this is the case in many scenarios), the performance of these approaches fall backs to the performance of DQN.

In this paper we propose to use cross-learner regularizers to prevent the collapse of the representation space in ensemble-based Q-learning methods. Intuitively, these representations capture an inductive bias towards more diverse representations. We have investigated five different regularizers. The mathematical formulation of four of the regularizers correspond to inequality measures borrowed from economics theory. While in economics, in general, high inequality is seen as a negative, in this case we use the metrics to encourage inequality between the representations. The fifth regularizer is inspired consensus optimization.

To summarize, our contributions are following:

1. We show that high representation similarity between neural network based Q-functions leads to decline in performance in ensemble based Q-learning methods.
2. To mitigate this, we propose five regularizers based on inequality measures from economics theory and consensus optimization that increase representation dissimilarity between Q-functions in ensemble based Q-learning methods.
3. We show that applying the proposed regularizers to the MaxminDQN and EnsembleDQN methods can lead to significant improvement in performance over a variety of benchmarks.

2 Background

Reinforcement learning considers an agent as a Markov Decision Process (MDP) defined as a five element tuple $(\mathcal{S}, \mathcal{A}, P, r, \gamma)$, where \mathcal{S} is the state space, \mathcal{A} is the action space, $P : \mathcal{S} \times \mathcal{A} \times \mathcal{S} \rightarrow [0, 1]$ are the state-action transition probabilities, $r : \mathcal{S} \times \mathcal{A} \times \mathcal{S} \rightarrow \mathbb{R}$ is the reward mapping and $\gamma \rightarrow [0, 1]$ is the discount factor. At each time step t the agent observes the state of the environment $s_t \in \mathcal{S}$ and selects an action $a_t \in \mathcal{A}$. The effect of the action triggers a transition to a new state $s_{t+1} \in \mathcal{S}$ according to the transition probabilities P , while the agent receives a scalar reward $R_t = r(s_t, a_t, s_{t+1})$. The goal of the agent is to learn a policy π that maximizes the expectation of the discounted sum of future rewards.

One way to implicitly learn the policy π is the Q-learning algorithm that estimates the expected sum of rewards of state s_t if we take the action a_t by solving the Bellman equation

$$Q^*(s_t, a_t) = \mathbb{E} \left[R_t + \max_{a' \in \mathcal{A}} Q^*(s_{t+1}, a') \right]$$

The implicit policy π can be extracted by acting greedily with respect to the optimal Q-function: $\operatorname{argmax}_{a \in \mathcal{A}} Q^*(s, a)$. One possible way to estimate the optimal Q-value is by iteratively updating it for sampled states s_t and action a_t using

$$Q^*(s_t, a_t) \leftarrow Q^*(s_t, a_t) + \alpha (Y_t - Q^*(s_t, a_t)) \quad \text{where } Y_t = R_t + \max_{a' \in \mathcal{A}} Q^*(s_{t+1}, a')$$

where α is the step size and Y_t is called the target value. While this algorithm had been initially studied in the context of a tabular representation of Q for discrete states and actions, in many practical applications the Q value is approximated by a learned function. Since the emergence of deep learning, the preferred approximation technique is based on a deep neural network. DQN [2], the first deep RL algorithm based on these ideas had demonstrated super-human performance in Atari Games, but required a very large number of training iterations. From this baseline, subsequent algorithms improved both the learning speed and achievable performance, with one of the main means for this being techniques to reduce the overestimation bias of the Q-function.

Ensemble DQN [10] uses an ensemble of N neural networks to estimate state-action values and uses their average to reduce both overestimation bias and estimation variance. Formally, the target value

for Ensemble DQN is calculated using

$$Q_E(\cdot) = \frac{1}{N} \sum_{i=1}^N Q_i(\cdot)$$

$$Y_t^E = R_t + \max_{a' \in \mathcal{A}} Q_E(s_{t+1}, a') \quad (1)$$

More recent, Maxmin DQN [11] addresses the overestimation bias using order statistics, using the ensemble size N as a hyperparameter to tune between underestimating and overestimating bias. The target value for Maxmin DQN is calculated using

$$Q_M(\cdot, \cdot) = \min_{i=1, \dots, N} Q_i(\cdot, \cdot)$$

$$Y_t^M = R_t + \max_{a' \in \mathcal{A}} Q_M(s_{t+1}, a') \quad (2)$$

3 Related Work

Techniques to Address Overestimation Bias in RL: Addressing overestimation bias is a long standing research topic not only in reinforcement learning but other fields of science such as economics and statistics. It is commonly known as *max-operator bias* in statistics [12] and as *the winner’s curse* in economics [13, 14]. As we already discussed above, the max operator in the Q-learning models naturally lead to overestimation bias. To address this, [4] proposed Double Q-learning, subsequently adapted to a neural network based function approximators as Double DQN [7]. Alternatively, [15, 16] proposed weighted estimators of Double Q-learning and [17] introduced a bias correction term. Other approaches to address the overestimation are based on averaging and ensembling. Techniques include averaging Q-values from previous N versions of the Q-network [10], taking linear combinations of min and max over the pool of Q-values [18], or using a random mixture from the pool [19].

Regularization in Reinforcement Learning: Regularization in reinforcement learning has been used to perform effective exploration and learning generalized policies. For instance, [20] uses mutual-information regularization to optimize a prior action distribution for better performance and exploration, [21] regularizes the policy $\pi(a|s)$ using a control prior, [22] uses temporal difference error regularization to reduce variance in Generalized Advantage Estimation [23]. Generalization in reinforcement learning refers to the performance of the policy on different environment compared to the training environment. For example, [24] studied the effect of L^2 norm on DQN on generalization, [25] studied generalization between simulations vs. the real world, [26] studied parameter variations and [27] studied the effect of different random seeds in environment generation.

Representation Similarity: Measuring similarity between the representations learned by different neural networks is an active area of research. For instance, [28] used Canonical Correlation Analysis (CCA) to measure the representation similarity. CCA find two basis matrices such that when original matrices are projected on these bases, the correlation is maximized. [28, 29] used truncated singular value decomposition on the activations to make it robust for perturbations. Other work such as [30] and [31] studied the correlation between the neurons in the neural networks. [30] attempts to find a bipartite match that maximizes the sum of correlations between the neurons. [31] proposed finding subsets of neurons such that neurons of one neural network can be represented as a linear combination of neurons from the second neural network.

4 Increasing Representation Dissimilarity in Ensemble-Based Deep Q-Learning

The work described in this paper is based on the conjecture that while ensemble-based deep Q-learning approaches aim to reduce the overestimation bias, this only works to the degree that the neural networks in the ensemble use different representations. If during training, these networks collapse to closely related representations, the learning performance decreases. From this idea, we propose to use regularization techniques to increase representation dissimilarity between the networks of the ensemble.

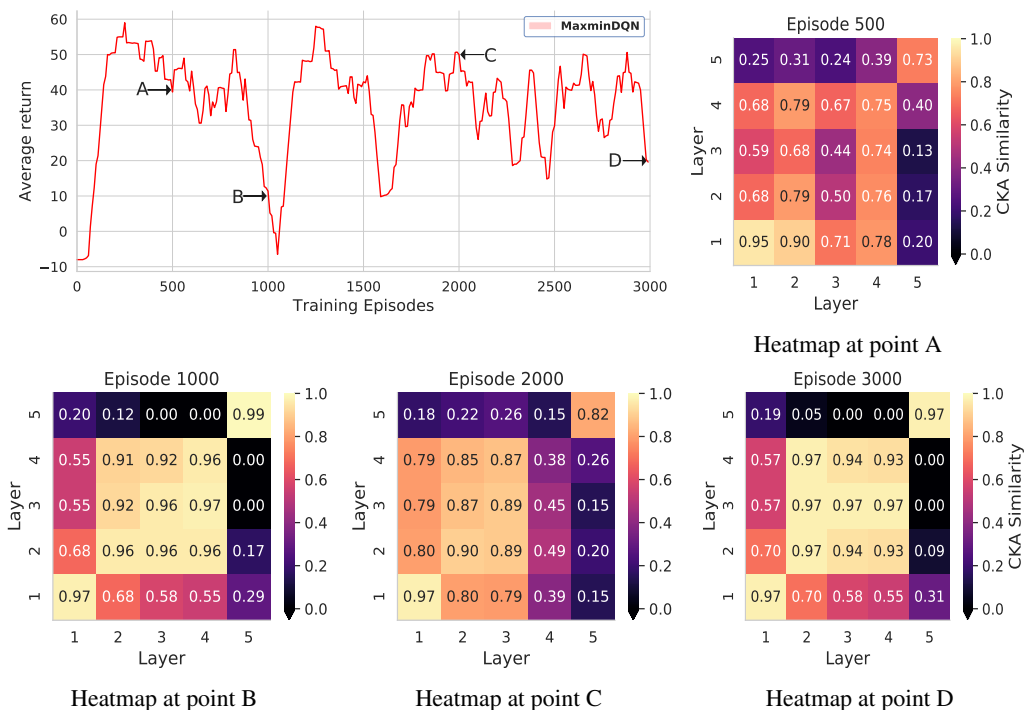


Figure 1: The training graph and CKA similarity heatmaps of a MaxminDQN agent with 2 neural networks. The letters on the plot show the time when CKA similarities were calculated. Heatmaps at A and C have relatively low CKA similarity and have relatively higher average return as compared to heatmaps at point B and D that have extremely high similarity across all the layers.

4.1 Representation Similarity Measure

Let $X \in \mathbb{R}^{n \times p_1}$ denote a matrix of activations of p_1 neurons for n examples and $Y \in \mathbb{R}^{n \times p_2}$ denote a matrix of activations of p_2 neurons for the same n examples. Furthermore, we consider $K_{ij} = k(x_i, x_j)$ and $L_{ij} = l(y_i, y_j)$ where k and l are two kernels.

Centered Kernel Alignment (CKA) [32, 33, 34] is a method for comparing representations of neural networks, and identifying correspondences between layers, not only in the same network but also on different neural network architectures. CKA is a normalized form of Hilbert-Schmidt Independence Criterion (HSIC) [35]. Formally, CKA is defined as:

$$\text{CKA}(K, L) = \frac{\text{HSIC}(K, L)}{\sqrt{\text{HSIC}(K, K) \cdot \text{HSIC}(L, L)}}$$

HSIC is a test statistic for determining whether two sets of variables are independent. The empirical estimator of HSIC is defined as:

$$\text{HSIC}(K, L) = \frac{1}{(n-1)^2} \text{tr}(KHLH)$$

where H is the centering matrix $H_n = I_n - \frac{1}{n}\mathbf{1}\mathbf{1}^T$.

In Appendix A.1, we performed a simple regression experiment to demonstrate that when two neural networks trained on same data, despite having different architecture, learning rate and batch size can learn almost identical representations.

4.2 Correlation Between Performance and Representation Similarity

The work in this paper starts from the conjecture that high representation similarity between neural networks in an ensemble-based Q-learning technique correlates to poor performance. To empirically

verify our hypothesis, we trained a MaxminDQN agent with two neural networks on the Catcher environment [36] for about 3000 episodes (5×10^6 training steps) and calculated the CKA similarity with a linear kernel after every 500 episodes. The training graph along with the CKA similarity heatmaps can be seen in Figure 1. Notably at episode 500 (heatmap A) and episode 2000 (heatmap C), the representation similarity between neural networks is low but the average return is relatively high. In contrast, at episode 1000 (heatmap B) and episode 3000 (heatmap D) the representation similarity is highest but the average return is lowest.

4.3 Regularization for Increasing Representation Dissimilarity

In order to increase the representation dissimilarity, we propose to regularize the training algorithm with an additional criteria that favors dissimilarity in the representation. There is no universally agreed metric for degree of dissimilarity, but a number of well-established metrics are used in different branches of science. We have experimented with five different metrics.

In the following, N is the number of neural networks in the ensemble, ℓ_i is the L^2 norm of the i -th neural network’s parameters, $\bar{\ell}$ is the mean of all the L^2 norms and ℓ is the list of all the L^2 norms.

The first four metrics we consider are based on inequality measures from economic theory. While in economics, inequality is usually considered something to be avoided, in our case we aim to increase inequality (and thus, representation dissimilarity).

The **Atkinson Index** [37] measures income inequality and is useful in identifying the end of the distribution that contributes the most towards the observed inequality. Formally, it is defined as

$$A_\epsilon = \begin{cases} 1 - \frac{1}{\bar{\ell}} \left(\frac{1}{N} \sum_{i=1}^N \ell_i^{1-\epsilon} \right)^{\frac{1}{1-\epsilon_{at}}}, & \text{for } 0 \leq \epsilon_{at} \neq 1, \\ 1 - \frac{1}{\bar{\ell}} \left(\frac{1}{N} \prod_{i=1}^N \ell_i \right)^{\frac{1}{N}}, & \text{for } \epsilon_{at} = 1, \end{cases} \quad (3)$$

where ϵ_{at} is the inequality aversion parameter used to tune the sensitivity of the measured change. When $\epsilon_{at} = 0$, the index is more sensitive to the changes at the upper end of the distribution, while the index becomes more sensitive towards the change at the lower end of the distribution when ϵ_{at} approaches 1.

The **Gini coefficient** [38] is a statistical measure of the wealth distribution or income inequality among a population and defined as the half of the relative mean absolute difference:

$$G = \frac{\sum_{i=1}^N \sum_{j=1}^N |\ell_i - \ell_j|}{2N^2 \bar{\ell}} \quad (4)$$

The Gini coefficient is more sensitive to deviation around the middle of the distribution than at the upper or lower part of the distribution.

The **Theil index** [39] measures redundancy, lack of diversity, isolation, segregation and income inequality among a population. Using the Theil index is identical to measuring the redundancy in information theory, defined as the maximum possible entropy of the data minus the observed entropy:

$$T_T = \frac{1}{N} \sum_{i=1}^N \frac{\ell_i}{\bar{\ell}} \ln \frac{\ell_i}{\bar{\ell}} \quad (5)$$

The **variance of logarithms** [40] is a widely used measure of dispersion with natural links to wage distribution models. Formally, it is defined as:

$$V_L(\ell) = \frac{1}{N} \sum_{i=1}^N [\ln \ell_i - \ln g(\ell)]^2 \quad (6)$$

where $g(\ell)$ is the geometric mean of ℓ defined as $(\prod_{i=1}^N \ell_i)^{1/N}$.

The final regularization method we use is inspired from consensus optimization. In a consensus method [41], a number of models are independently optimized with their own task-specific parameters,

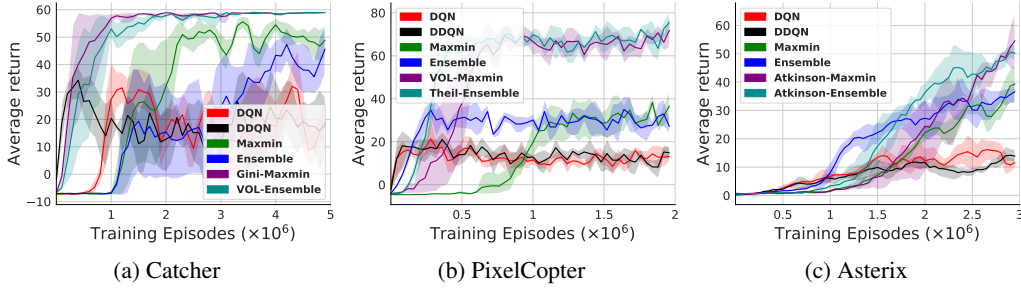


Figure 2: Training curves and 95% confidence interval (shaded area) for the best augmented variants for Maxmin and Ensemble together with baseline algorithms.

and the tasks communicate via a penalty that encourages all the individual solutions to converge around a common value. Formally, it is defined as

$$M = \|\bar{\ell} - \ell_i\|^2 \quad (7)$$

We will refer this regularizer as MeanVector throughout this paper.

4.4 Training Algorithm

Using the regularization functions defined above, we can develop diversity-regularized variants of the the MaxminDQN and EnsembleDQN algorithms. The training technique is identical to the algorithms described in [11] and [10], with a regularization term added to the loss of the Q-functions. The loss term for i -th Q-function with parameters ψ_i is:

$$\mathcal{L}(\psi_i) = \mathbb{E}_{s,a,r,s'} \left[(Q_{\psi}^i(s,a) - Y)^2 \right] - \lambda \mathcal{I}(\ell_i, \ell),$$

where Y is the target value calculated using either Equation (1) or Equation (2) depending on the algorithm, \mathcal{I} is the regularizer of choice from the list above and λ is the regularization weight. Notice that the regularization term appears with a negative sign, as the regularizers are essentially inequality metrics that we want to maximize instead of minimizing. For completeness, the algorithm can be found in Appendix B.

5 Experiments

5.1 Training Curves

To investigate the impact of the proposed regularization approach, we chose three environments from PyGames[36] and MinAtar [42]: Catcher, Pixelcopter and Asterix. We reused all the hyper-parameter settings from [11] except the number of neural networks, which we limited to four and trained each solution for five fixed seeds. For the regularization weight λ , we chose the best value from $\{10^{-5}, 10^{-6}, 10^{-7}, 10^{-8}\}$. The complete list of training parameters can be found in Appendix E.

Figure 2 shows the training curves for the three environments. To avoid crowding the figures, for each environment and baseline algorithm (MaxminDQN and EnsembleDQN) we only plotted the regularized version which performed the best. We also show as baseline the original MaxminDQN and EnsembleDQN, as well as the DQN and DDQN algorithms. For the Catcher environment, both Gini-MaxminDQN and VOL-EnsembleDQN were able to quickly reach the optimal performance and stabilized after 2×10^6 training steps while the baseline MaxminDQN reached its maximum performance after 3.5×10^6 training steps but went down afterwards. Similarly, the baseline EnsembleDQN reached its maximum performance after 4×10^6 training steps, with the performance fluctuating with continued training. For the PixelCopter environment, VOL-MaxminDQN and Theil-EnsembleDQN were slower in the initial part of the learning that some of the other approaches, but over time they achieved at least double return compared to the other approaches. Similarly, for the Asterix environment, Atkinson-MaxminDQN and Atkinson-EnsembleDQN lagged in training for about 1×10^6 training steps but after that they achieved at least 50% higher return compared to the baselined. Full results together with CKA similarity heatmaps are found in Appendix C.

5.2 t-SNE Visualizations

To visualize the impact of the dissimilarity regularization, Figure 3 shows t-SNE [43] visualization of the activations of the last layer of the trained networks. Figure 3a show the network trained for the Catcher environment, while Figure 3b, the network trained for the PixelCopter environment. The upper row of the figure shows the original, unregularized models, while the lower row a regularized version. For all combinations, we find that the activations from the original MaxminDQN and EnsembleDQN versions do not show any obvious pattern, while the regularized ones show distinct clusters. An additional benefit of t-SNE visualizations over CKA similarity heatmaps is that the CKA similarity heatmaps are useful to show representation similarity between two neural networks, but they become counter intuitive as the number of neural networks increases. More t-SNE visualizations for four neural network experiments can be seen in Appendix C.3.

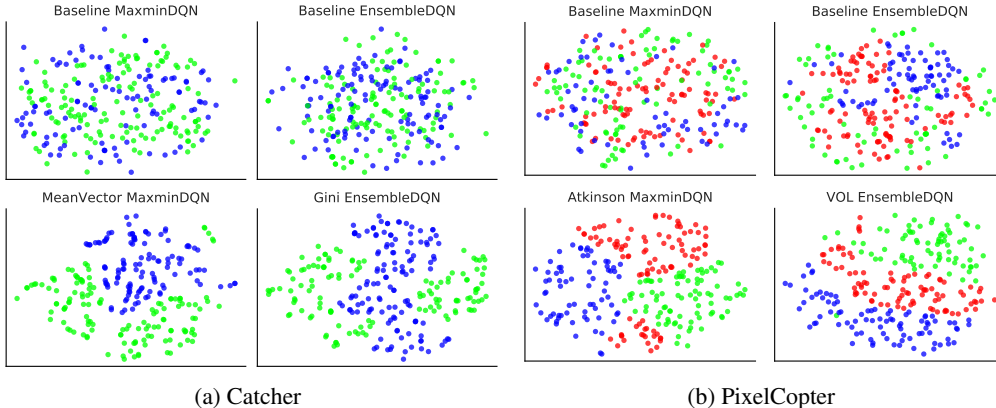


Figure 3: Clustering last layer activations from Catcher and PixelCopter after processing them with t-SNE to map them in 2D.

5.3 Statistical Analysis

What is the impact of the regularization on the performance? Similarly to the approach taken by [44], to rigorously evaluate the improvement of regularization over baseline solutions, we performed a z -score test. The z -score is also known as “standard score”, the signed fractional number of standard deviations by which the value of a data point is above the mean value. A regularizer’s z -score roughly measures its relative performance among others. For each algorithm, environment and neural network setting, we calculated the z -score for each regularization method and the baseline by treating results all the results as a populations. For example, to find out which EnsembleDQN with two neural networks is best for the Catcher environment, we took the average reward of 10 episodes for each experiment $((5 + 1) \times 5$ seeds) and treated it as a population. Finally, we averaged the z -scores of all five seeds to generate the final result presented in Table 1. In terms of improved performance, almost all the regularizers have achieved significant improvement over the baselines for all three environments. The only example where a regularized model was worse than the baseline was for the Theil-MaxminDQN and MeanVector-MaxminDQN models with three neural networks on the Asterix environment. The z -scores for four neural network experiments can be found Appendix C.4.

Is the improvement statistically significant? We collected the z -scores from the previous section and performed the Welch’s t -test (two-sample t -test with unequal variance) with the corresponding z -scores produced by the baseline. The resulting p -values are presented in Table 2. From the results, we observed that the improvement introduced from regularization are statistically significant ($p < 0.05$) in almost all the cases except for MaxminDQN with three neural networks for the Asterix environment.

Table 1: Averaged z -scores for each regularization method.

Reg	Ensemble N=2			Maxmin N=2			Ensemble N=3			Maxmin N=3		
	Catcher	Copter	Asterix									
Baseline	-2.125	-2.044	-1.758	-2.143	-2.031	-1.957	-1.931	-2.042	-1.738	-1.702	-2.115	-0.244
Atkinson	0.419	0.450	0.006	0.353	0.402	0.744	0.379	0.292	0.627	0.344	0.380	0.640
Gini	0.422	0.563	0.659	0.539	0.446	0.290	0.349	0.231	0.531	0.319	0.624	0.419
MeanVector	0.426	0.359	0.564	0.529	0.079	0.121	0.403	0.763	0.300	0.347	0.316	-0.350
Theil	0.425	0.358	0.265	0.198	0.576	0.06	0.402	0.284	0.132	0.341	0.499	-0.371
VOL	0.433	0.315	0.263	0.522	0.526	0.741	0.397	0.471	0.149	0.35	0.297	-0.093

Table 2: P -values from Welch’s t -test comparing the z -scores of regularization and baseline

Reg	Ensemble N=2			Maxmin N=2			Ensemble N=3			Maxmin N=3		
	Catcher	Copter	Asterix	Catcher	Copter	Asterix	Catcher	Copter	Asterix	Catcher	Copter	Asterix
Atkinson	0.002	0.000	0.010	0.000	0.000	0.004	0.019	0.000	0.004	0.061	0.000	0.409
Gini	0.002	0.000	0.064	0.000	0.000	0.011	0.002	0.003	0.004	0.061	0.000	0.409
MeanVector	0.002	0.000	0.012	0.000	0.008	0.015	0.019	0.000	0.037	0.061	0.000	0.931
Theil	0.002	0.002	0.013	0.000	0.000	0.011	0.019	0.001	0.083	0.061	0.001	0.913
VOL	0.002	0.000	0.006	0.000	0.005	0.004	0.019	0.000	0.065	0.060	0.000	0.866

5.4 Identical Layers Experiment

To test the limits of the regularizers, we initialized, each layer of each neural network with the same fixed seed. We performed this experiment on all three environments and used the exact same seeds and hyperparameters that were used for the main experiments. The training curves can be seen in Figure 4. Notably, the results from the baseline MaxminDQN and EnsembleDQN on both Catcher and PixelCopter environments are similar to the main results. For the Catcher environment, both Gini-MaxminDQN and Theil-EnsembleDQN were slow in learning for about 2×10^6 training steps but both solutions were able to achieve the optimal performance by the end of training. Similarly for PixelCopter environment, the VOL-MaxminDQN was slow in learning till 1.5×10^6 training steps but it was able to outperform the baseline results and achieved results similar to the main experiments. The complete training plots for these experiments can be seen in Appendix D.

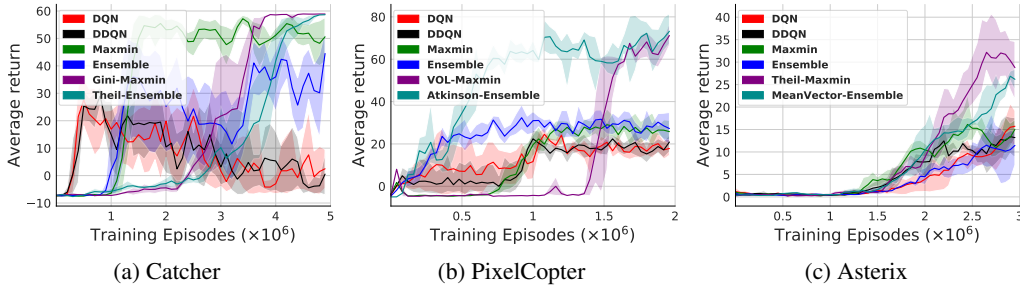


Figure 4: Training plots representing the best results from each solution for Catcher, PixelCopter and Asterix environment when the layers of the neural networks were initialized with one fixed seed.

6 Conclusion

In this paper we showed that high representation similarity between the Q-functions in ensemble based Q-learning algorithms such as MaxminDQN and EnsembleDQN leads to a decline in learning performance. To mitigate this, we proposed a regularization approach using five different metrics to increase the dissimilarity in the representation space of the Q-functions. Experiments have shown that our solution outperforms baseline MaxminDQN and EnsembleDQN in standard training settings as well as in scenarios where the parameters of the neural layers were initialized using one fixed seed.

Broader impacts

Deep RL algorithms brought a significant intellectual ferment to the AI community, due to their ability to achieve super-human performance in a number of benchmarks. Unfortunately, many of the benchmarks that established the Deep RL algorithms are gaming environments where a large number of reinforcement runs can be performed comparatively cheaply. The general consensus remains that, in the general case, deep RL algorithms are several performance and learning speed breakthroughs away from deployment in the physical world. This paper proposes regularization techniques that can be applied to ensemble based Q-learning algorithms, which can lead to significant performance and learning speed increases. For instance, in many scenarios the achieved return is about double compared with the unregularized baselines, and this performance is achieved, in many cases, significantly faster. Thus, the proposed approach might be one of the necessary steps towards the real-world deployment of the deep RL algorithms.

References

- [1] Chris Watkins. *Learning from Delayed Rewards*. PhD thesis, King’s College, Cambridge, 1989.
- [2] Volodymyr Mnih, Koray Kavukcuoglu, David Silver, Andrei A. Rusu, Joel Veness, Marc G. Bellemare, Alex Graves, Martin Riedmiller, Andreas K. Fidjeland, Georg Ostrovski, Stig Petersen, Charles Beattie, Amir Sadik, Ioannis Antonoglou, Helen King, Dharmashan Kumaran, Daan Wierstra, Shane Legg, and Demis Hassabis. Human-level control through deep reinforcement learning. *Nature*, 518(7540):529–533, February 2015.
- [3] Sebastian Thrun and A. Schwartz. Issues in using function approximation for reinforcement learning. In *Proceedings of the Connectionist Models Summer School (CMSS-1993)*, January 1993.
- [4] Hado van Hasselt. Double Q-learning. In *Proceedings of the Advances in Neural Information Processing Systems (NIPS-2010)*, pages 2613–2621, 2010.
- [5] István Szita and András Lőrincz. The Many Faces of Optimism: A Unifying Approach. In *Proceedings of International Conference on Machine Learning (ICML-2008)*, pages 1048–1055, 2008.
- [6] Alexander L. Strehl, Lihong Li, and Michael L. Littman. Reinforcement Learning in Finite MDPs: PAC Analysis. *Journal of Machine Learning Research (JMLR)*, 10(Nov):2413–2444, 2009.
- [7] Hado van Hasselt, Arthur Guez, and David Silver. Deep Reinforcement Learning with Double Q-learning. In *Proceeding of Conference on Artificial Intelligence (AAAI-2016)*, 2016.
- [8] Scott Fujimoto, Herke Van Hoof, and David Meger. Addressing function approximation error in actor-critic methods. *arXiv preprint arXiv:1802.09477*, 2018.
- [9] Tuomas Haarnoja, Aurick Zhou, Pieter Abbeel, and Sergey Levine. Soft actor-critic: Off-policy maximum entropy deep reinforcement learning with a stochastic actor. *arXiv preprint arXiv:1801.01290*, 2018.
- [10] Oron Anschel, Nir Baram, and Nahum Shimkin. Averaged-DQN: Variance reduction and stabilization for deep reinforcement learning. In *Proceedings of the International Conference on Machine Learning (ICML-2017)*, pages 176–185, 2017.
- [11] Qingfeng Lan, Yangchen Pan, Alona Fyshe, and Martha White. Maxmin Q-learning: Controlling the estimation bias of Q-learning. In *Proceeding of the International Conference on Learning Representations (ICLR-2020)*, 2020.
- [12] Carlo D’Eramo, Alessandro Nuara, Matteo Pirodda, and Marcello Restelli. Estimating the maximum expected value in continuous reinforcement learning problems. In *Proceedings of the Conference on Artificial Intelligence (AAAI-2017)*, 2017.
- [13] Richard Thaler. *The winner’s curse: Paradoxes and anomalies of economic life*. 2012.
- [14] James E Smith and Robert L Winkler. The optimizer’s curse: Skepticism and postdecision surprise in decision analysis. *Management Science*, 52(3):311–322, 2006.
- [15] Zongzhang Zhang, Zhiyuan Pan, and Mykel J Kochenderfer. Weighted double Q-learning. In *Proceedings of the International Joint Conferences on Artificial Intelligence (IJCAI-2017)*, pages 3455–3461, 2017.
- [16] P. Lv, X. Wang, Y. Cheng, and Z. Duan. Stochastic double deep q-network. *IEEE Access*, 7:79446–79454, 2019.
- [17] Donghun Lee, Boris Defourny, and Warren B. Powell. Bias-corrected Q-learning to Control Max-operator Bias in Q-learning. In *IEEE Symposium on Adaptive Dynamic Programming and Reinforcement Learning*, pages 93–99, 2013.
- [18] Aviral Kumar, Justin Fu, Matthew Soh, George Tucker, and Sergey Levine. Stabilizing off-policy Q-learning via bootstrapping error reduction. In *Proceedings of the Advances in Neural Information Processing Systems (NeurIPS-2019)*, pages 11761–11771, 2019.

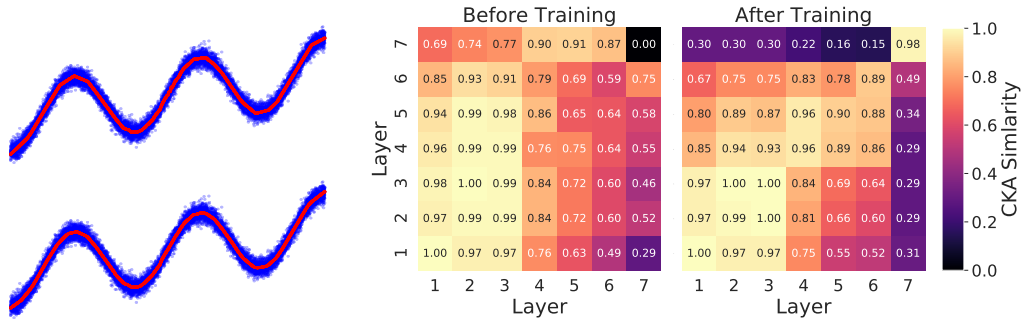
- [19] Rishabh Agarwal, Dale Schuurmans, and Mohammad Norouzi. Striving for simplicity in off-policy deep reinforcement learning. *arXiv preprint arXiv:1907.04543*, 2019.
- [20] Jordi Grau-Moya, Felix Leibfried, and Peter Vrancx. Soft Q-learning with mutual-information regularization. In *Proceedings of the International Conference on Learning Representations (ICLR-2019)*, 2019.
- [21] Richard Cheng, Abhinav Verma, Gbor Orosz, Swarat Chaudhuri, Yisong Yue, and Joel Burdick. Control regularization for reduced variance reinforcement learning. *arXiv preprint arXiv:1905.05380*, 2019.
- [22] Alexandre Galashov, Siddhant Jayakumar, Leonard Hasenclever, Dhruva Tirumala, Jonathan Schwarz, Guillaume Desjardins, Wojciech Czarnecki, Yee Whye Teh, Razvan Pascanu, and Nicolas Heess. Information asymmetry in KL-regularized RL. In *Proceedings of the International Conference on Learning Representation (ICLR-2019)*, 2019.
- [23] John Schulman, Philipp Moritz, Sergey Levine, Michael Jordan, and Pieter Abbeel. High-dimensional continuous control using generalized advantage estimation. In *Proceedings of the International Conference on Learning Representations (ICLR-2016)*, 2016.
- [24] Jesse Farebrother, Marlos C. Machado, and Michael Bowling. Generalization and regularization in DQN, 2018.
- [25] Josh Tobin, Rachel Fong, Alex Ray, Jonas Schneider, Wojciech Zaremba, and Pieter Abbeel. Domain randomization for transferring deep neural networks from simulation to the real world. In *Proceedings of the International Conference on Intelligent Robots and Systems (IROS-2017)*, pages 23–30, 2017.
- [26] Anay Pattanaik, Zhenyi Tang, Shuijing Liu, Gautham Bommanan, and Girish Chowdhary. Robust deep reinforcement learning with adversarial attacks. In *Proceedings of the International Conference on Autonomous Agents and MultiAgent Systems (AAMAS-2018)*, pages 2040–2042, 2018.
- [27] Chiyuan Zhang, Oriol Vinyals, Remi Munos, and Samy Bengio. A study on overfitting in deep reinforcement learning. *arXiv preprint arXiv:1804.06893*, 2018.
- [28] Maithra Raghu, Justin Gilmer, Jason Yosinski, and Jascha Sohl-Dickstein. Svcca: Singular vector canonical correlation analysis for deep learning dynamics and interpretability. In *Proceedings of the Advances in Neural Information Processing Systems (NIPS-2017)*, pages 6076–6085. 2017.
- [29] Youssef Mroueh, Etienne Marcheret, and Vaibhava Goel. Multimodal retrieval with asymmetrically weighted truncated-svd canonical correlation analysis. *CoRR*, abs/1511.06267, 2015.
- [30] Yixuan Li, Jason Yosinski, Jeff Clune, Hod Lipson, and John Hopcroft. Convergent learning: Do different neural networks learn the same representations? In *Proceedings of the International Workshop on Feature Extraction: Modern Questions and Challenges at NIPS 2015*, volume 44, pages 196–212, 2015.
- [31] Liwei Wang, Lunjia Hu, Jiayuan Gu, Zhiqiang Hu, Yue Wu, Kun He, and John Hopcroft. Towards understanding learning representations: To what extent do different neural networks learn the same representation. In *Proceedings of the Advances in Neural Information Processing Systems (NIPS-2018)*, pages 9584–9593, 2018.
- [32] Simon Kornblith, Mohammad Norouzi, Honglak Lee, and Geoffrey Hinton. Similarity of neural network representations revisited. In *Proceedings of the International Conference on Machine Learning (ICML-2019)*, pages 3519–3529, 09–15 Jun 2019.
- [33] Corinna Cortes, Mehryar Mohri, and Afshin Rostamizadeh. Algorithms for learning kernels based on centered alignment. *Journal of Machine Learning Research*, 13(Mar):795–828, 2012.
- [34] Nello Cristianini, John Shawe-Taylor, Andre Elisseeff, and Jaz S Kandola. On kernel-target alignment. In *Proceedings of the Advances in Neural Information Processing Systems (NIPS-2002)*, pages 367–373, 2002.
- [35] Arthur Gretton, Olivier Bousquet, Alex Smola, and Bernhard Schölkopf. Measuring statistical dependence with hilbert-schmidt norms. In *Algorithmic Learning Theory (ALT)*, pages 63–77, 2005.
- [36] Lan Qingfeng. Gym compatible games for reinforcenment learning. <https://github.com/qlan3/gym-games>, 2019.
- [37] Anthony B Atkinson et al. On the measurement of inequality. *Journal of economic theory*, 2(3):244–263, 1970.
- [38] Paul D. Allison. Measures of inequality. *American Sociological Review*, 43(6):865–880, 1978.
- [39] J. Johnston. H. Theil. Economics and Information Theory. *The Economic Journal*, 79(315):601–602, 09 1969.
- [40] Efe A. Ok and James Foster. Lorenz Dominance and the Variance of Logarithms. Working Papers 97-22, C.V. Starr Center for Applied Economics, New York University, 1997.

- [41] Stephen Boyd, Neal Parikh, Eric Chu, Borja Peleato, and Jonathan Eckstein. Distributed optimization and statistical learning via the alternating direction method of multipliers. *Foundations and Trends in Machine Learning*, 3(1):1–122, 2011.
- [42] Kenny Young and Tian Tian. Minatar: An atari-inspired testbed for thorough and reproducible reinforcement learning experiments. *arXiv preprint arXiv:1903.03176*, 2019.
- [43] Laurens van der Maaten and Geoffrey Hinton. Visualizing data using t-SNE. *Journal of Machine Learning Research*, 9:2579–2605, 2008.
- [44] Zhuang Liu, Xuanlin Li, Bingyi Kang, and Trevor Darrell. Regularization matters in policy optimization. *arXiv preprint arXiv:1910.09191*, 2020.

A Supplementary Material

A.1 Motivating Example to Demonstrate Similarity Between Neural Networks

We performed a regression experiment in which we learnt a sine wave function using two different three layered fully connected neural networks with 64 and 32 neurons in each hidden layer with ReLU. The neural networks were initialized using different seeds and were trained using different batch sizes (512, 128) and learning rates ($1e-4$, $1e-3$). The Figure 5a shows the learnt functions while Figure 5b represents their CKA similarity heatmap before and after training. The odd numbered layers represent pre-ReLU activations while the even numbered layers represent post-ReLU activations. It can be seen that before training, the CKA similarity between the two neural networks from layer 4 and onward is relatively low and the output being 0% similar while after training, the trained networks have learnt highly similar representation while their output being 98% similar.



(a) Regression using two different neural networks (b) CKA similarity heatmap between different layers of the two neural networks used for the regression experiment.

Figure 5: **Left:** Fitting a sine function using two different neural network architectures. The upper function was approximated using 64 neurons in each hidden layer while the lower function used 32 neurons in each hidden layer. **Right:** Represents the CKA similarity heatmap between different layers of both neural networks before and after training. The right diagonal (bottom left to top right) measures representation similarity of the corresponding layers of both neural networks. The trained networks have learnt similar representations while their output was 98% similar.

This example shows that neural networks can learn similar representation while trained on different batches. This observation is important because in MaxminDQN and EnsembleDQN training, each neural network is trained on a separate batch from the replay buffer but still learns similar representation similarity (see Figure 8).

B Algorithms

For completeness, the regularized MaxminDQN and EnsembleDQN algorithms are given below

Algorithm 1: Regularized MaxminDQN

The differences between the baseline MaxminDQN and regularized MaxminDQN are [highlighted](#)

Initialize N Q-functions $\{Q^1, \dots, Q^N\}$ parameterized by $\{\psi_1, \dots, \psi_N\}$

Initialize empty replay buffer D

Observe initial state s

while Agent is interacting with the Environment **do**

$Q^{min}(s, a) \leftarrow \min_{k \in \{1, \dots, N\}} Q^k(s, a), \forall a \in \mathcal{A}$

Choose action a by ϵ -greedy based on Q^{min}

Take action a , observe r, s'

Store transition (s, a, r, s') in D

Select a subset S from $\{1, \dots, N\}$ (e.g., randomly select one i to update)

for $i \in S$ **do**

Sample random mini-batch of transitions (s_D, a_D, r_D, s'_D) from D

Get update target: $Y^M \leftarrow r_D + \gamma \max_{a' \in \mathcal{A}} Q^{min}(s'_D, a')$

Generate list of L^2 norms : $\ell = [\|\psi_1\|^2, \dots, \|\psi_N\|^2]$

Update Q^i by minimizing $\mathbb{E}_{s_D, a_D, r_D, s'_D} \left(Q_{\psi_i}^i(s_D, a_D) - Y^M \right)^2 - \lambda \mathcal{I}(\ell_i, \ell)$

end

$s \leftarrow s'$

end

Algorithm 2: Regularized EnsembleDQN

The differences between the baseline EnsembleDQN and regularized EnsembleDQN are [highlighted](#)

Initialize N Q-functions $\{Q^1, \dots, Q^N\}$ parameterized by $\{\psi_1, \dots, \psi_N\}$

Initialize empty replay buffer D

Observe initial state s

while Agent is interacting with the Environment **do**

$Q^{ens}(s, a) \leftarrow \frac{1}{N} \sum_{i=1}^N Q^i(s, a)$

Choose action a by ϵ -greedy based on Q^{ens}

Take action a , observe r, s'

Store transition (s, a, r, s') in D

Select a subset S from $\{1, \dots, N\}$ (e.g., randomly select one i to update)

for $i \in S$ **do**

Sample random mini-batch of transitions (s_D, a_D, r_D, s'_D) from D

Get update target: $Y^E \leftarrow r_D + \gamma \max_{a' \in \mathcal{A}} Q^{ens}(s'_D, a')$

Generate list of L^2 norms : $\ell = [\|\psi_1\|^2, \dots, \|\psi_N\|^2]$

Update Q^i by minimizing $\mathbb{E}_{s_D, a_D, r_D, s'_D} \left(Q_{\psi_i}^i(s_D, a_D) - Y^E \right)^2 - \lambda \mathcal{I}(\ell_i, \ell)$

end

$s \leftarrow s'$

end

C All Training Plots

C.1 Training Plots for MaxminDQN

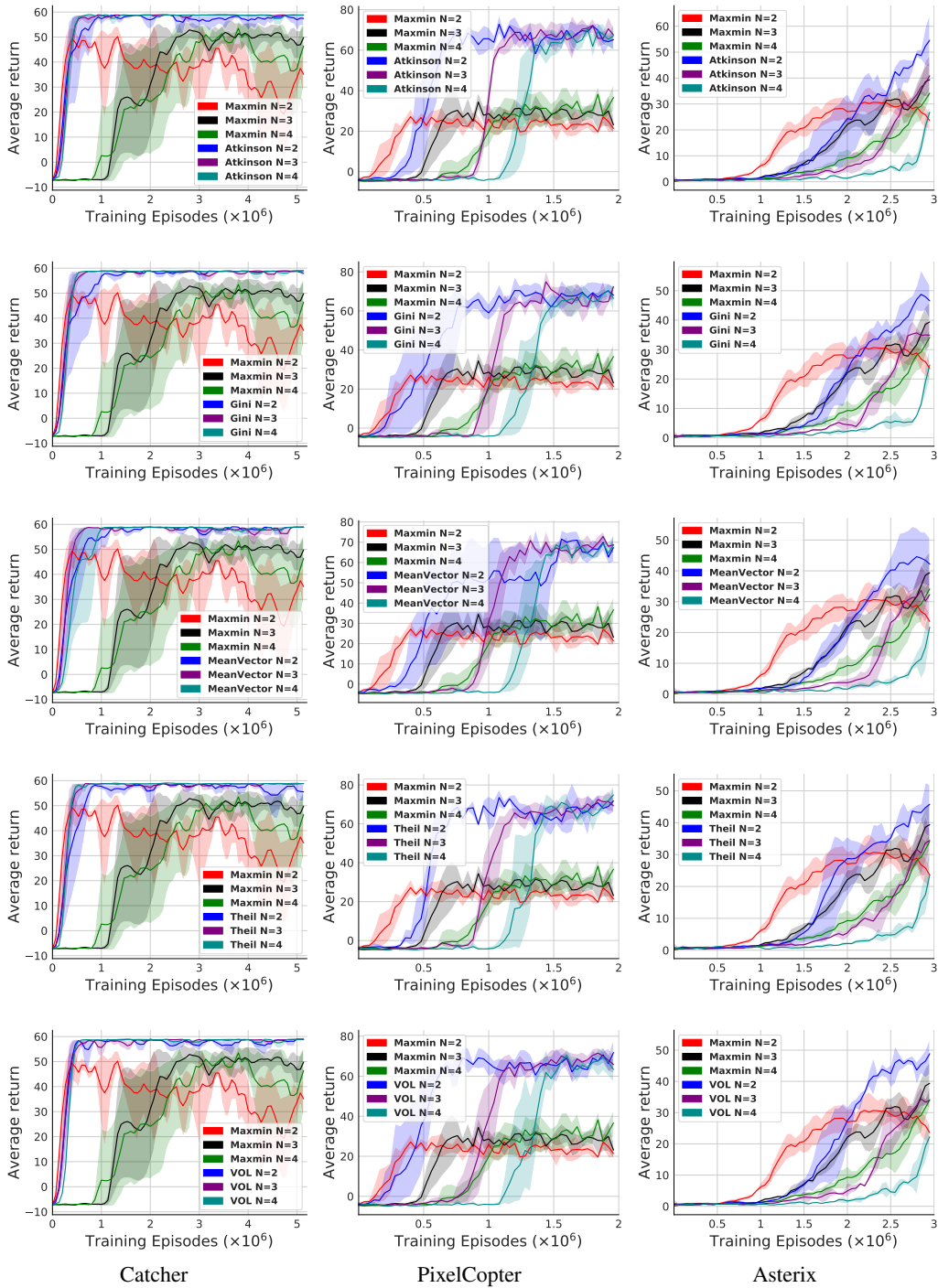


Figure 6: All MaxminDQN Results. Top to Bottom: Baseline, Atkinson, Gini, MeanVector, Theil, Variance of Logarithms

C.2 Training Plots for EnsembleDQN

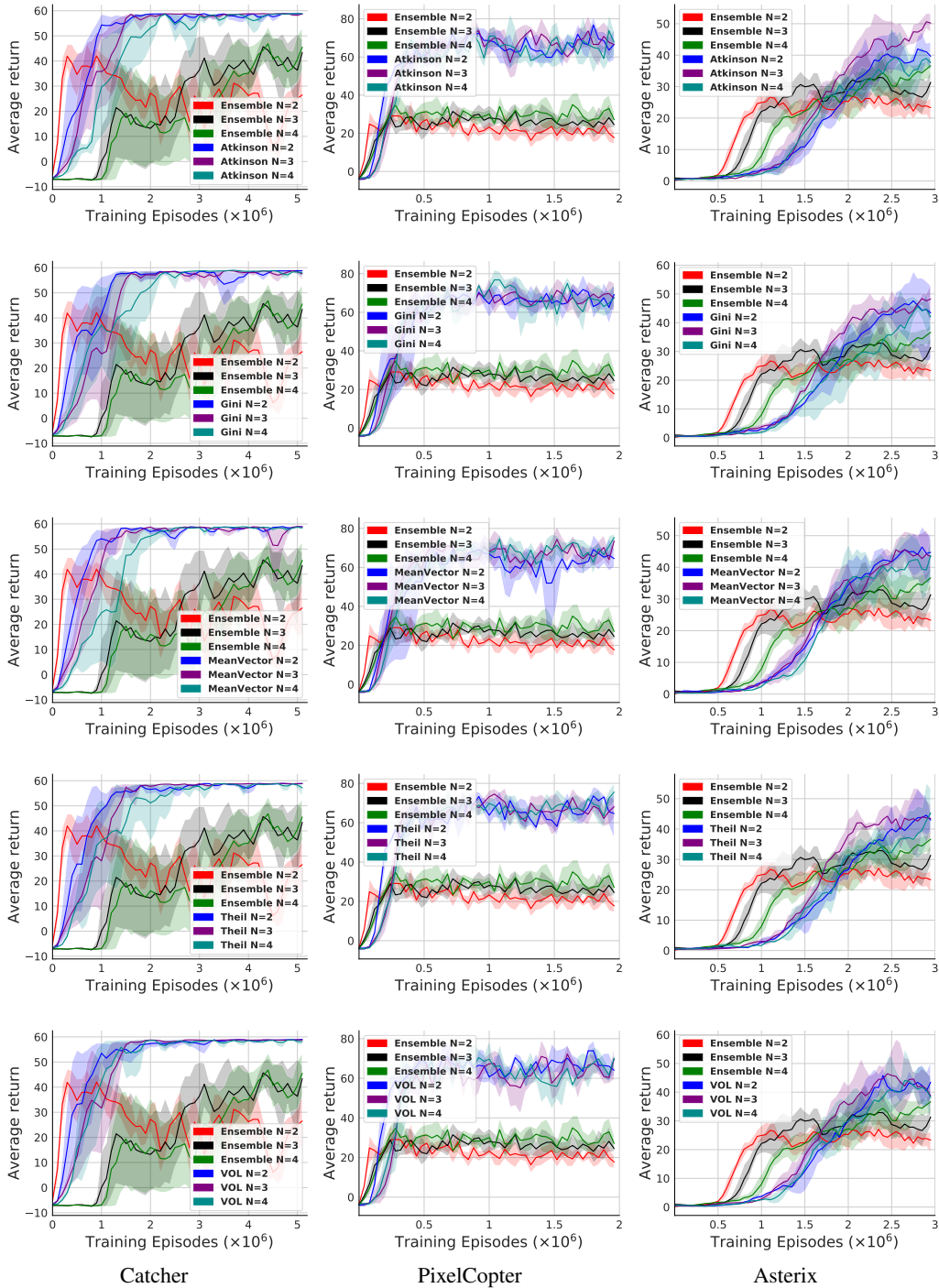


Figure 7: All EnsembleDQN Results. Top to Bottom: Baseline, Atkinson, Gini, MeanVector, Theil, Variance of Logarithms

C.3 Heatmaps and t-SNE Visualizations

Figure 8 represents the CKA similarity heatmaps using a linear kernel of all the two neural network experiments after training averaged over all the five seeds. The point of interest is the right diagonal (bottom left to top right) that represents the representation similarity between corresponding layers. For the baseline experiments, the output layer has more than 96% similarity in almost all the scenarios while for the regularized versions have around 90% similarity in the output layer. This 10% difference provides enough variance in the Q-values to prevent the ensemble based Q-learning methods converging to the standard DQN.

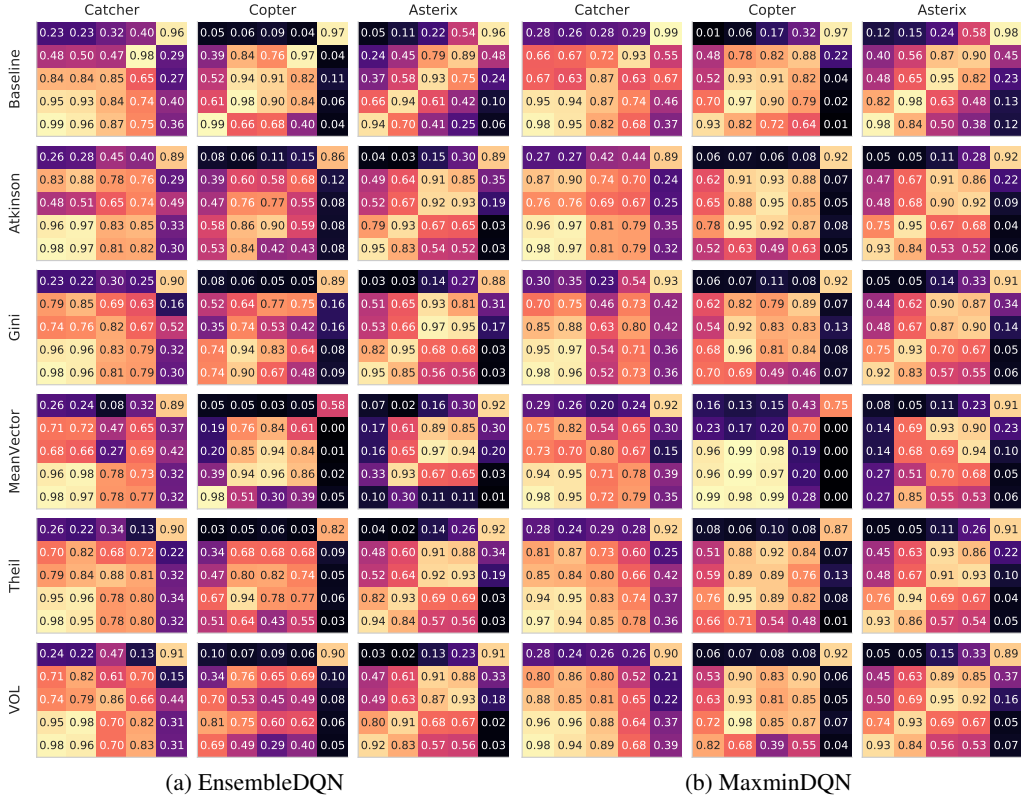


Figure 8: Heatmaps representing the CKA similarity of 2 neural network experiments.

Figure 9 represents the t-SNE visualizations of the baseline and regularized solutions trained with four neural networks on the PixelCopter environment. This visualization is consistent with the visualizations shown in Section 5.2 where the baseline activations are cluttered without any pattern while the Theil-MaxminDQN and Theil-EnsembleDQN activations have visible clusters.

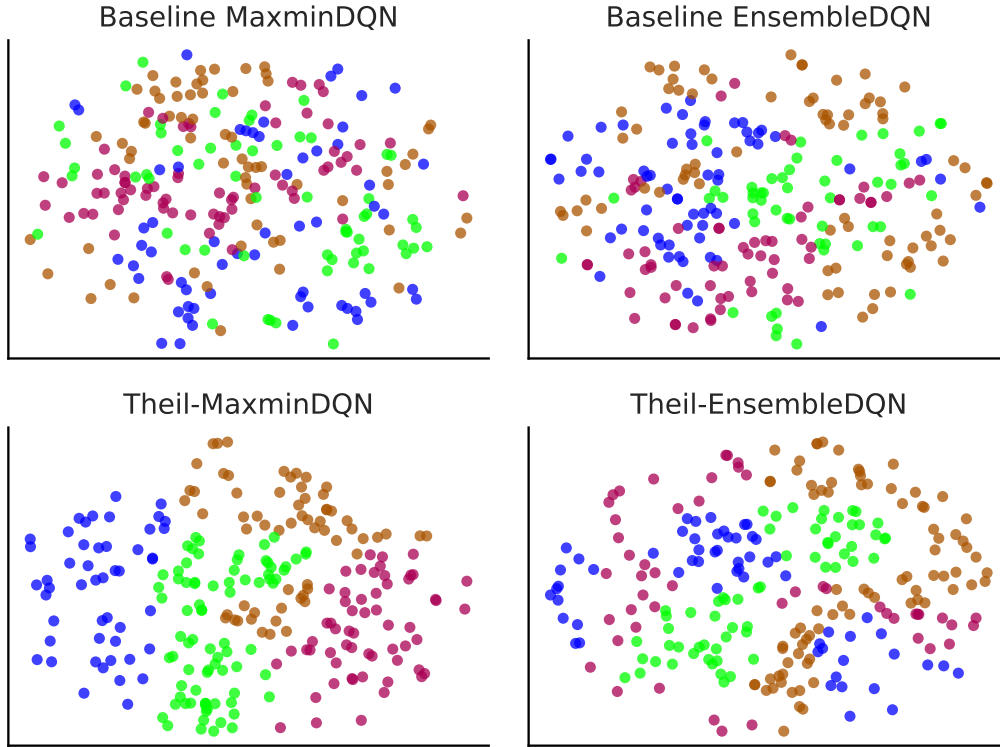


Figure 9: Clustering last layer activations from PixelCopter after processing them with t-SNE to map them in 2D

C.4 z-Score Table for Four Neural Network Experiments

Table 3: Averaged z-scores for each regularization method with four neural networks

Reg	Ensemble N=4			Maxmin N=4		
	Catcher	Copter	Asterix	Catcher	Copter	Asterix
Baseline	-2.096	-2.154	-1.061	-1.785	-1.803	1.242
Atkinson	0.486	0.146	-0.202	0.358	0.479	0.245
Gini	0.409	0.307	0.456	0.340	0.433	-0.189
MeanVector	0.452	0.685	0.366	0.362	0.206	-0.630
Theil	0.341	0.669	-0.032	0.363	0.842	-0.352
VOL	0.409	0.374	0.473	0.363	-0.167	-0.316

Table 4: P-values from Welch’s t-test comparing the z-scores of regularization and baseline

Reg	Ensemble N=4			Maxmin N=4		
	Catcher	Copter	Asterix	Catcher	Copter	Asterix
Atkinson	0.002	0.005	0.345	0.044	0.018	0.319
Gini	0.002	0.005	0.126	0.045	0.024	0.180
MeanVector	0.002	0.000	0.157	0.044	0.010	0.116
Theil	0.001	0.001	0.265	0.044	0.005	0.180
VOL	0.002	0.003	0.126	0.044	0.024	0.151

D All Training Plots for Identical Layered Experiments

D.1 Training Plots for MaxminDQN

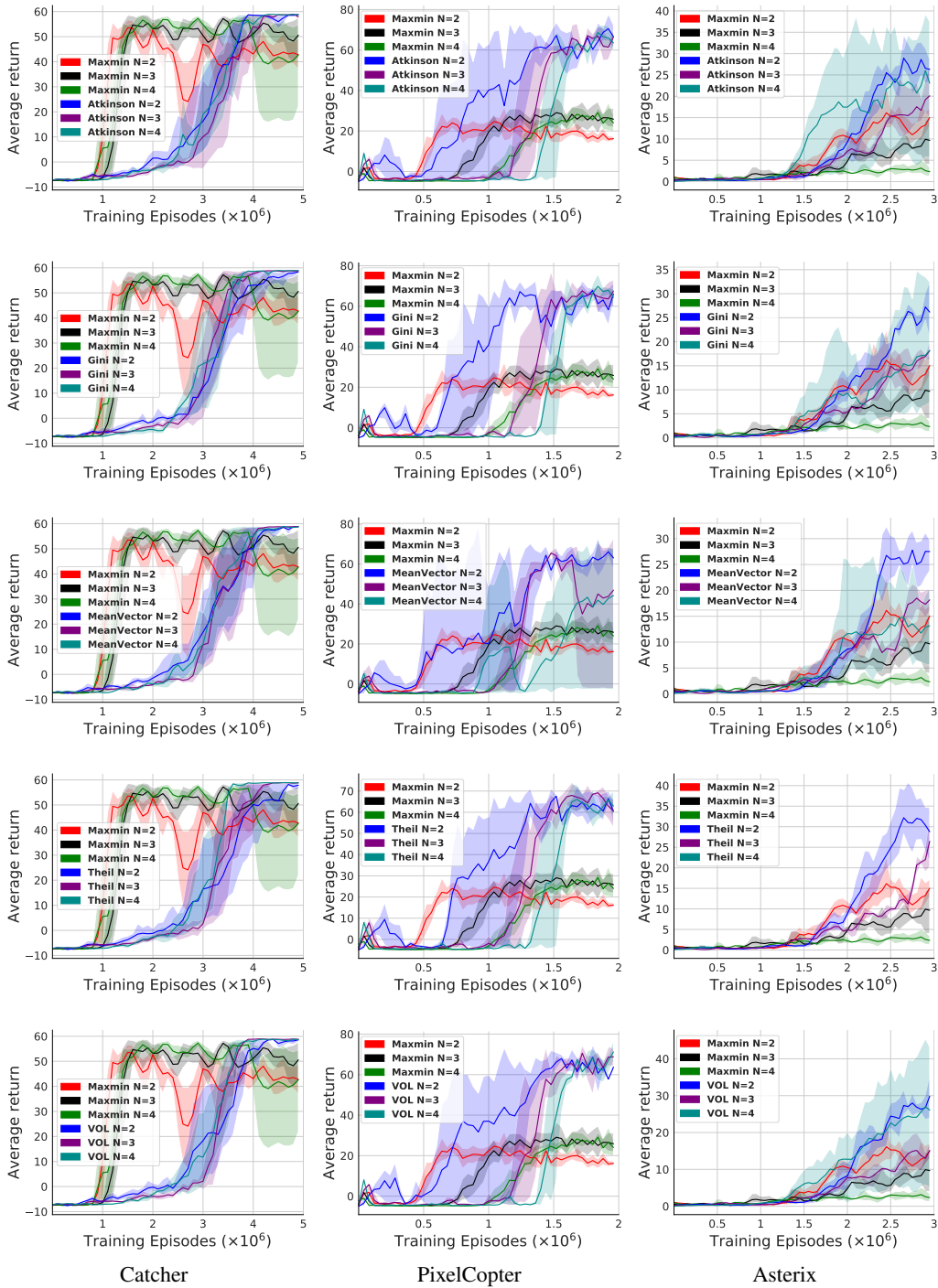


Figure 10: All MaxminDQN Results. Top to Bottom: Baseline, Atkinson, Gini, MeanVector, Theil, Variance of Logarithms

D.2 Training Plots for EnsembleDQN

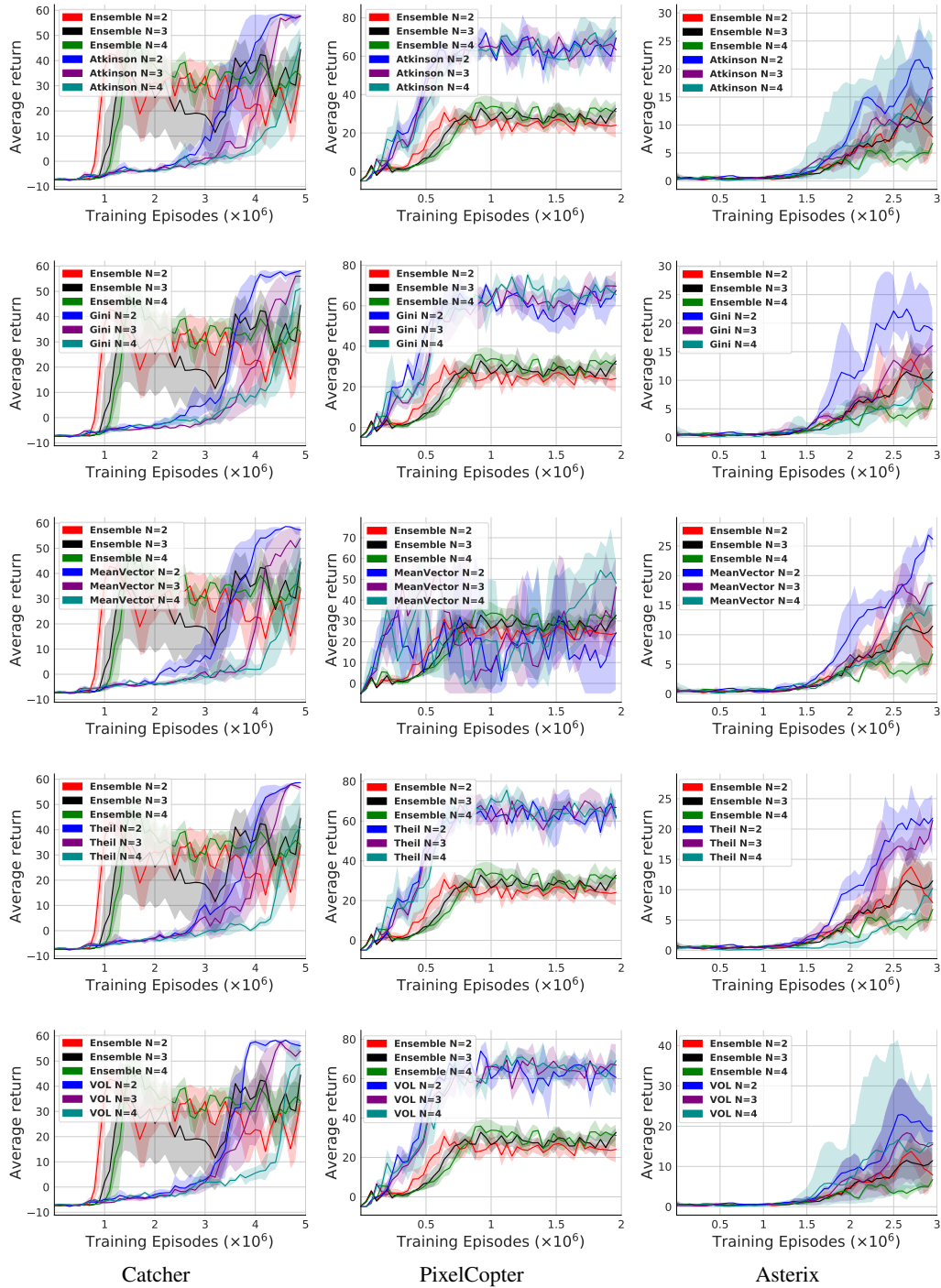


Figure 11: All EnsembleDQN Results. Top to Bottom: Baseline, Atkinson, Gini, MeanVector, Theil, Variance of Logarithms

E Implementation Details and Hyperparameters

For our implementation of MaxminDQN and EnsembleDQN we used the code provided by the MaxminDQN authors that has implementations of different DQN based methods (github.com/qlan3/Explorer). For the baseline experiments, we used most of the hyperparameter settings provided in the configuration files by the authors except learning rates which we limited to $[1e-3, 1e-4, 3e-5]$ and limited the number of ensembles to four. The complete list of hyperparameters for each environment is shown in Table 5. The values in bold represent the values used for the reported results.

Table 5: List of hyperparameters used for the experiments.

Hyperparameter	Catcher	PixelCopter	Asterix
Learning rate	$[1e-3, 1e-4, 3e-5]$	$[1e-3, 1e-4, 3e-5]$	$[1e-3, 1e-4, 3e-5]$
Batch size	[32, 64]	[32, 128, 1024]	[32, 64]
Buffer Size	$[1e4, 1e7]$	$[1e4, 1e6]$	$[1e5, 2e5]$
Exploration Steps	1e3	$[1e3, 2e3]$	2e5
Hidden Layer Size	[64, 64]	[64, 64]	[64, 64]
Gradient Clip	5	5	-1
Discount Factor γ	0.99	0.99	0.99
Regularization Weight	$[1e-5, 1e-6]$	$[1e-6, 1e-7, 1e-8]$	$[1e-5, 1e-6]$

For the identical layer experiment, no hyperparameter tuning was performed and we reused the hyperparameters from the main results. In terms of number of experiments, we ran 190 experiments: (5 regularizers \times 5 seeds \times 3 ensemble settings \times 2 algorithms) + 40 baseline experiments for each environment totaling 570 runs for all environments after hyperparameter tuning. The same number of experiments were performed for the identical layer experiment which sums up to 1140 runs where each run took 11 hours of compute time on average.

F Plotting the L^2 Norm Inequality

We measured the L^2 norm inequality of the baseline MaxminDQN and EnsembleDQN along with their regularized versions. We trained baseline MaxminDQN and EnsembleDQN with two neural networks along with their Gini index versions with regularization weight of $1e-8$ on the PixelCopter environment on a fixed seed. Figure 12 represents the L^2 norm inequality of the experiments along their average return during training. Notably, despite each neural network being trained on a different batch, the L^2 norm of the baseline MaxminDQN and EnsembleDQN are quite similar while the L^2 norm of the regularized MaxminDQN and EnsembleDQN have high inequality.

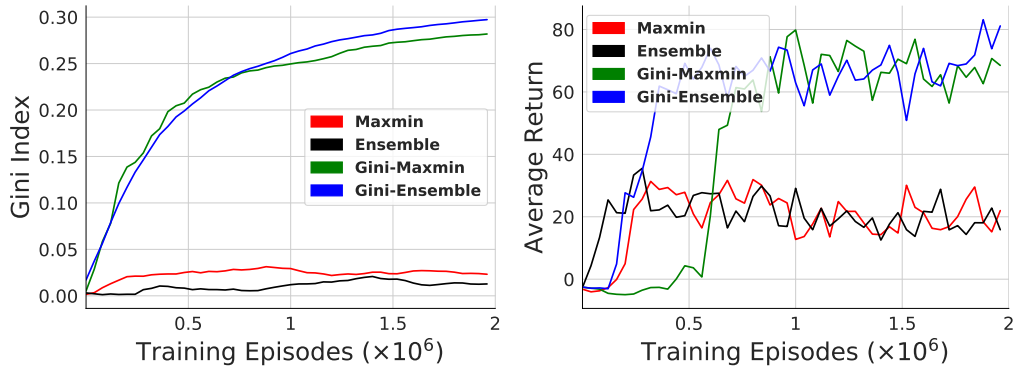


Figure 12: **Left:** Plot representing the L^2 norm inequality between the two neural networks using Gini index trained on PixelCopter environment. **Right:** Plot representing the average return during training.